Supplementary Materials

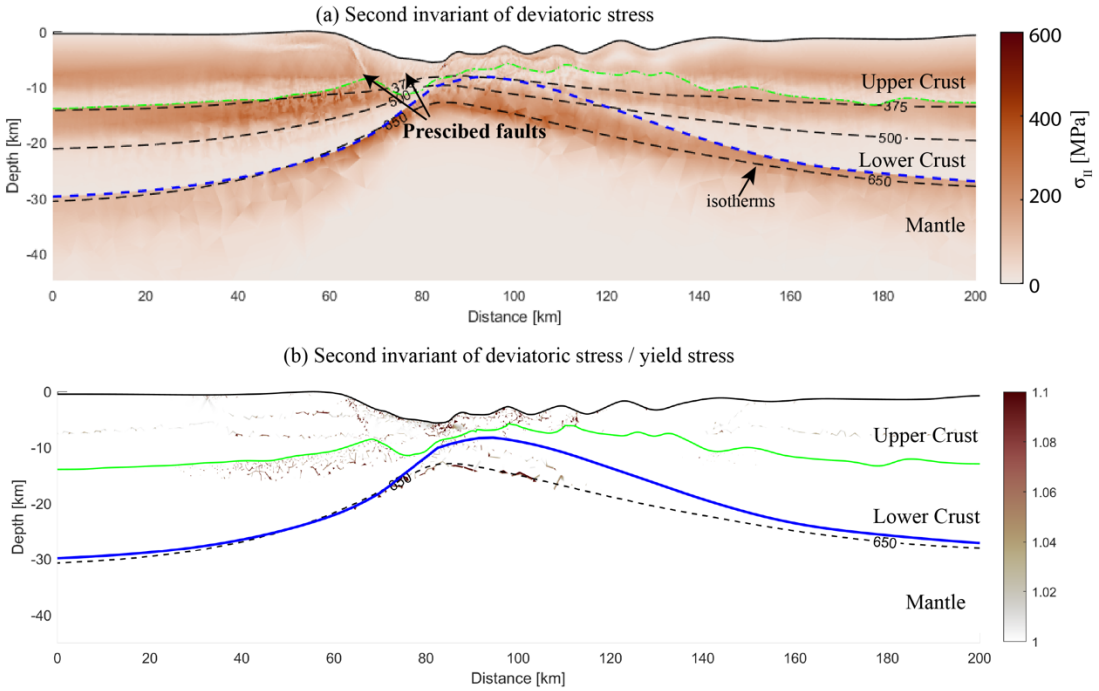

Fig. S1. Deviatoric stress of reference model (Fig.5). In the kinematic-dynamic mode of our model we inhibit plasticity in the upper crust outside the prescribed faults. This is done to promote slip along the observed faults in the seismic profile. Here we show that the deviatoric stress of the model, after several kinematically prescribed faults have functioned has reasonable values, see (a); and that the ratio of deviatoric stress to yield stress (as defined in eqs (5) and (8) in the Appendix), is, in general, lower than 1 and only in few locations reaches values up to ~1.1 (b). This specially occurs in the rift center, where only one main fault and a smaller conjugate fault have been prescribed. Including a larger number of small faults in the upper crust in those areas, would not change the main model architecture, but would decrease the deviatoric stress. Those small faults are not appreciated in seismic data, and probably occur in nature at sub-seismic scale. Their inclusion would not affect our results.

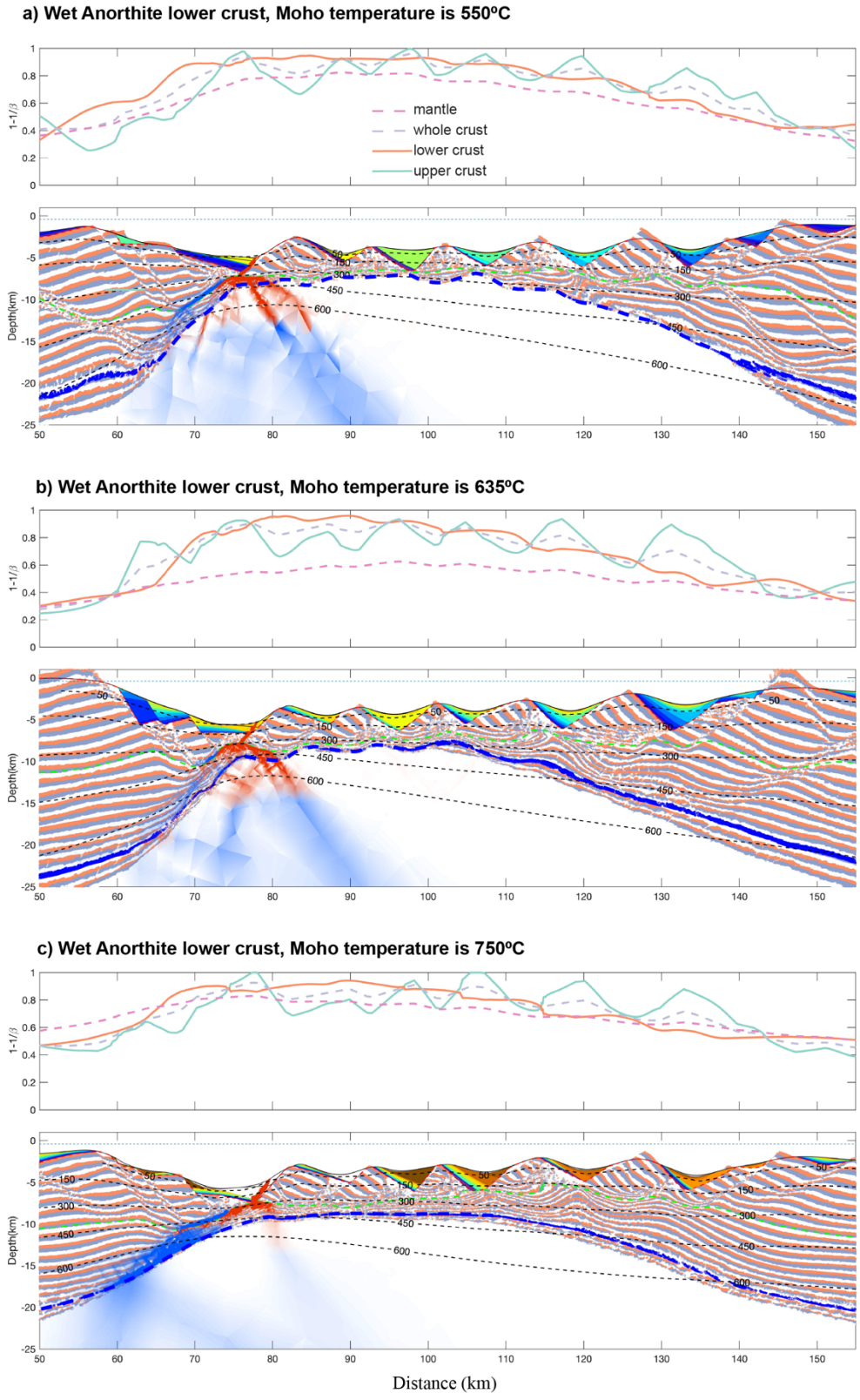

Fig. S2. Effect of different Moho temperatures on margin structure. Here we compare the result of modelling using three different Moho temperatures. For this modelling we use the same rheology parameters, geometry configuration and fault kinematics but different Moho temperatures by changing radiogenic heat production in the lower crust.

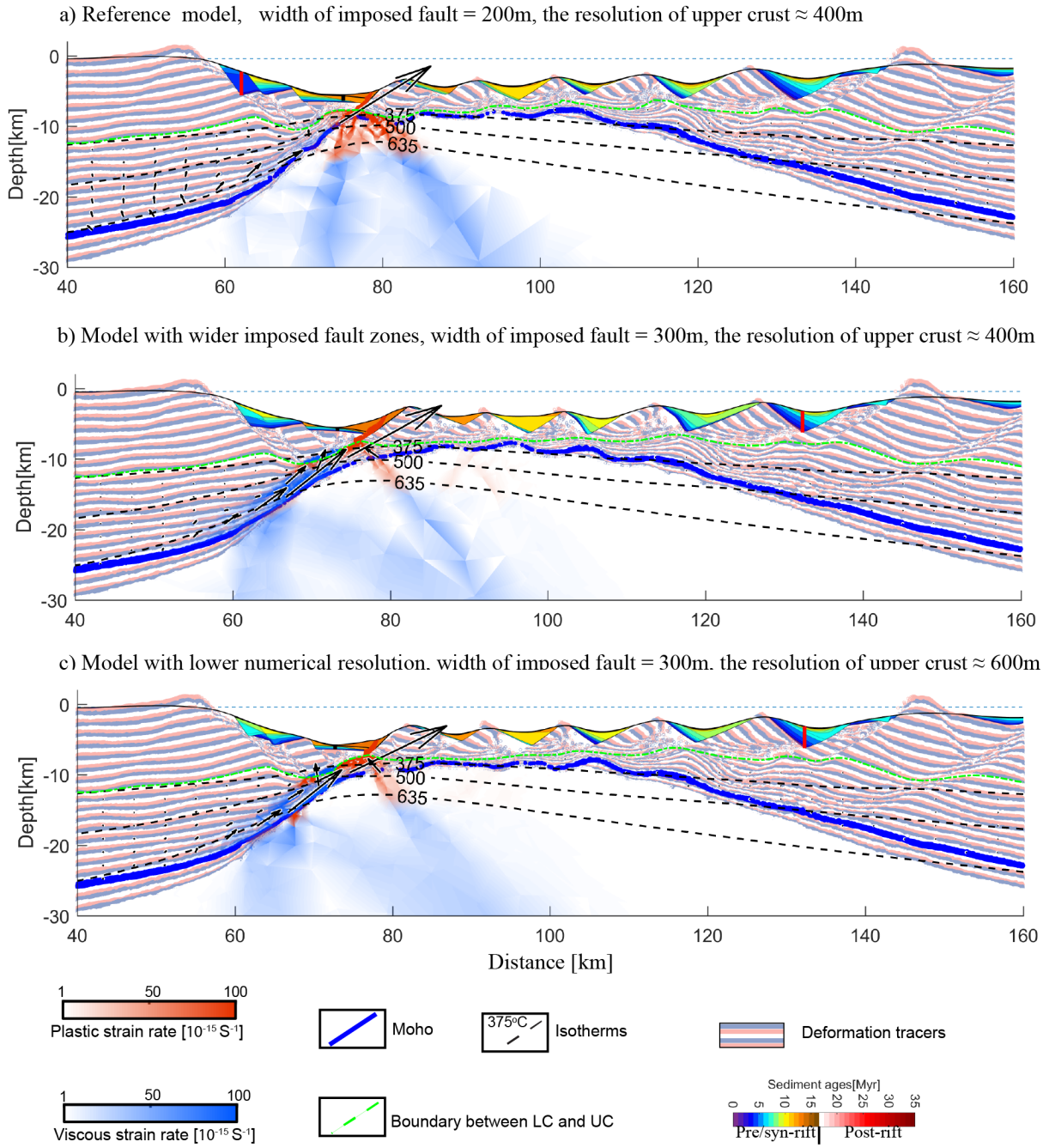

Fig. S3. Effect of numerical resolution. Within the parameters we have checked here, the resolution has a small effect on the margin structure. However, a higher numerical resolution, or a reduction in the fault width, would allow the model to show more detailed features, such as the undulation of the Moho.

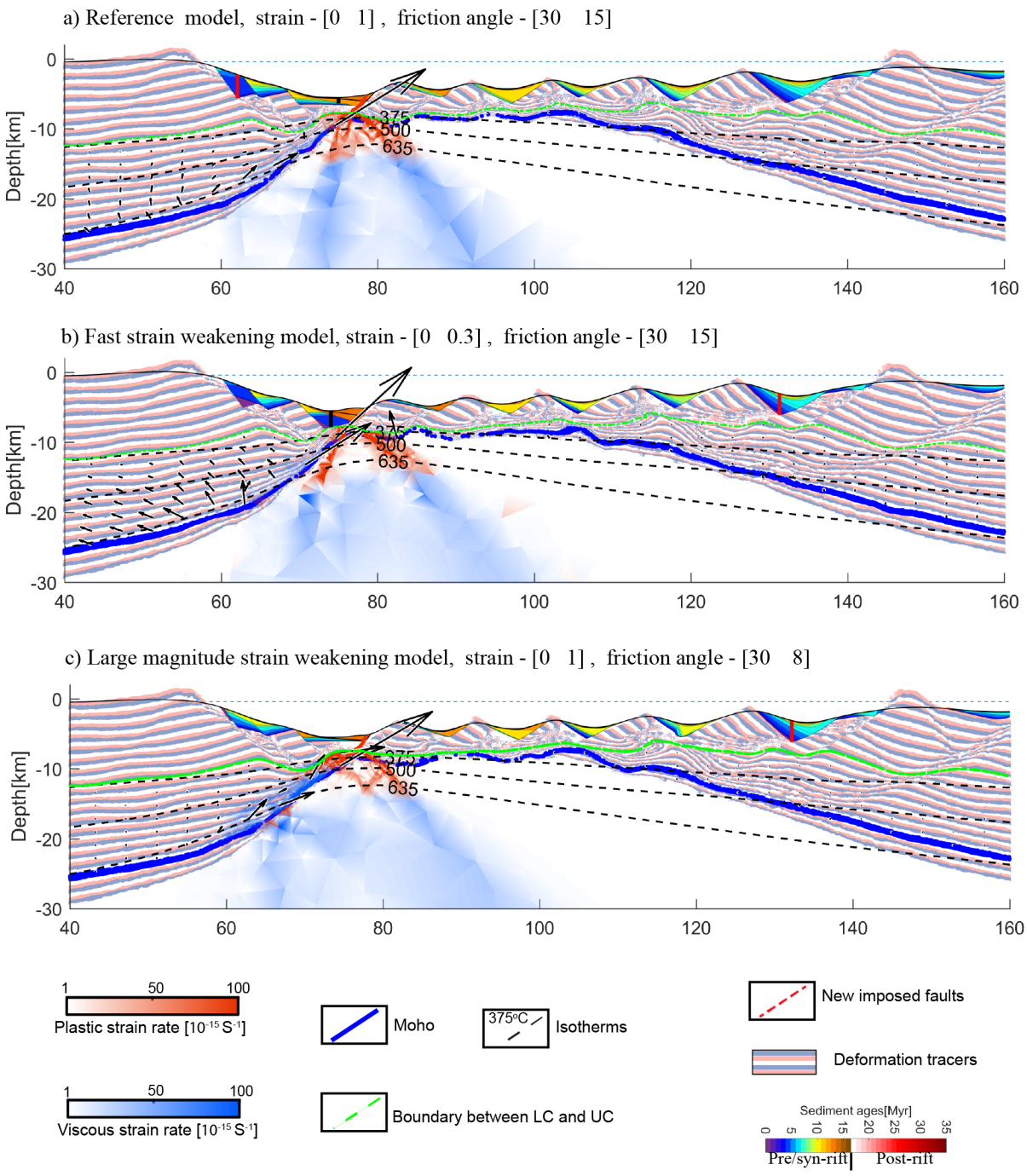

Fig. S4. Effect of rate and magnitude of strain weakening. From the results, it appears that these parameters have very little influence on the structure of the continental margin during the kinematic-dynamic simulation phase. As the deformation of the upper crust is mainly influenced by the kinematic fault during the kinematic - dynamic phase, these parameters have relatively small effect. For a discussion of the effect of these parameters on the results of the pure forward dynamic model, the reader is referred to previous studies, e.g. Naliboff et al 2017.

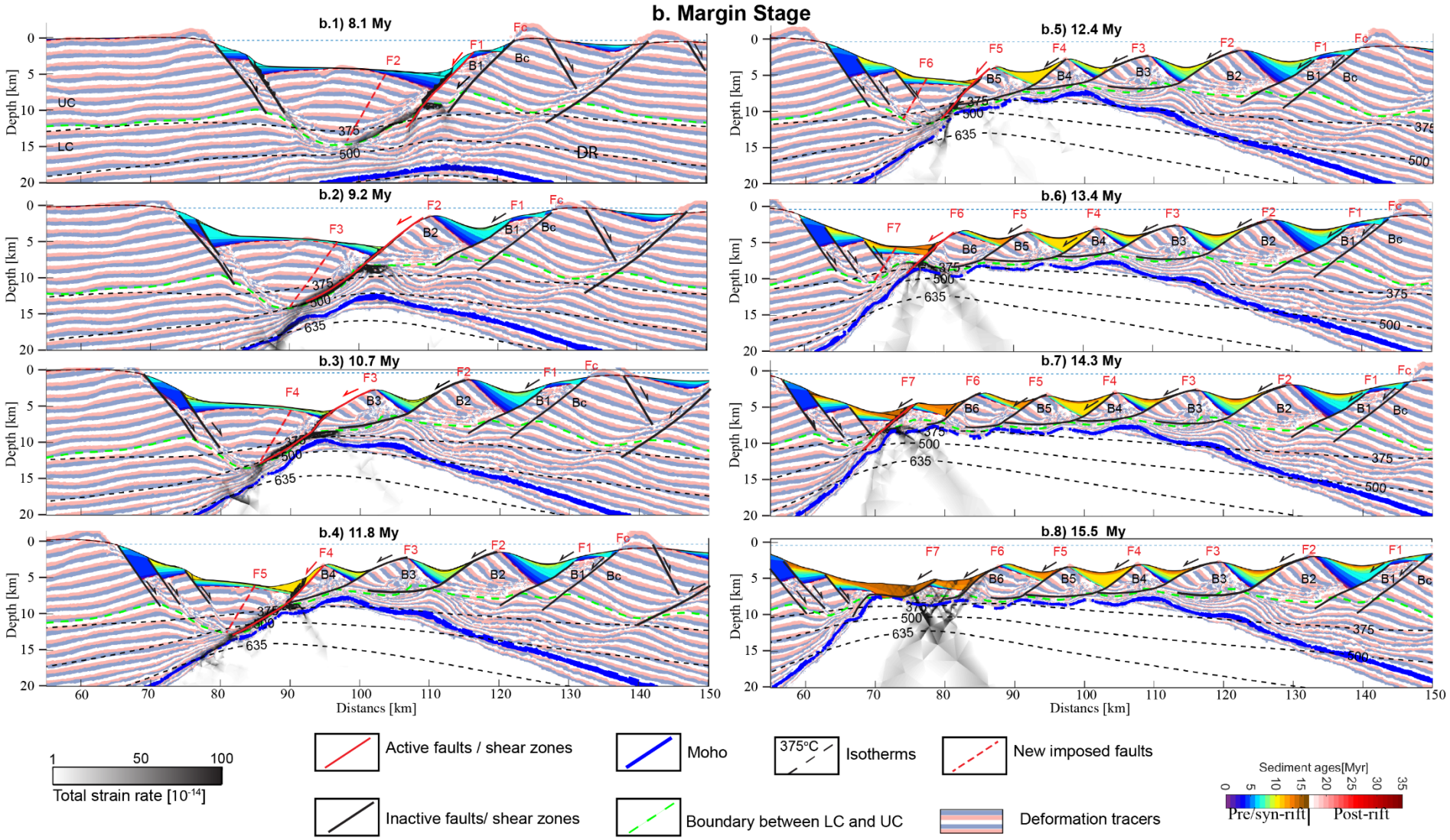

Fig.S5. The total strain rate at last time step of each active fault. The axis of maximum total strain rate is used to mark the fault/shear zone plane. Note that the range of strain rates shown here (10^{-14}-10^{-12}) is different with the one shown in Fig. 5 (10^{-15}-10^{-13}). The purpose of this change is to mark the high strain rate zone.

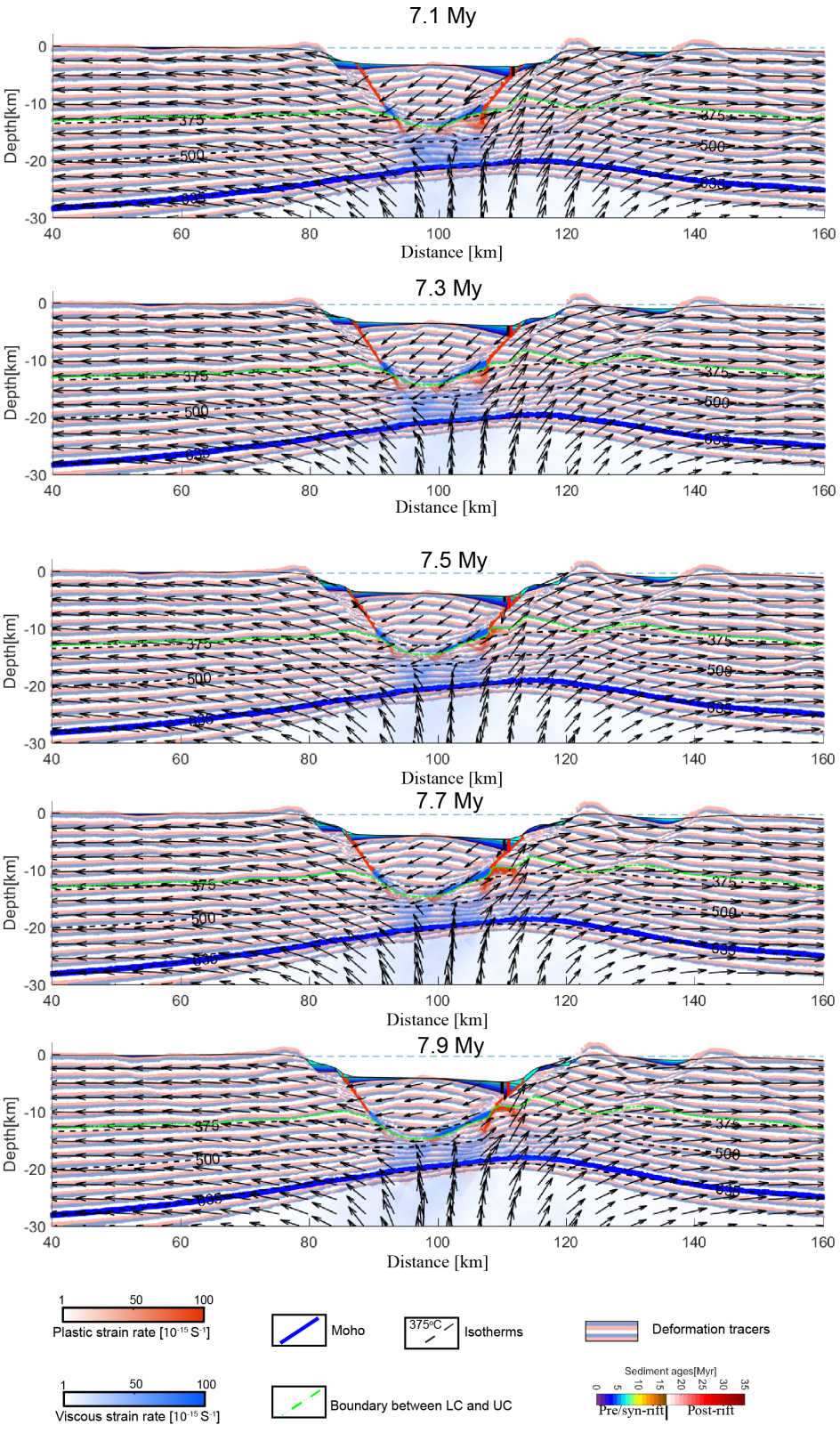

Fig. S6. Shows the evolution of F1. The black arrow shows the velocity vector, the slip rate over the imposed fault is determined by its position and the stress state of the system and is not imposed**.**

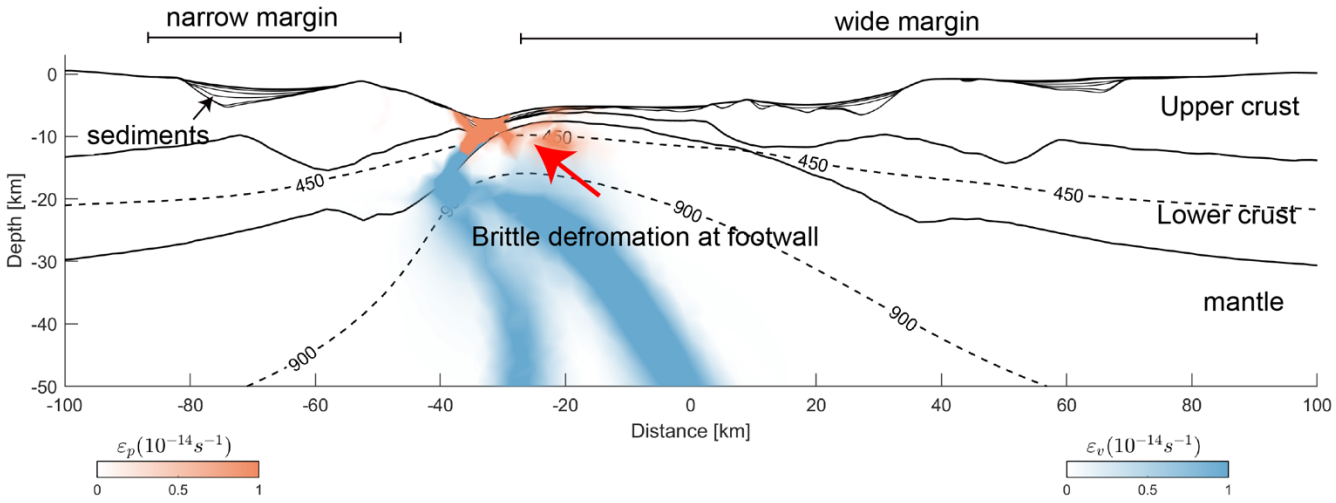

Fig. S7. Pure forward model with the similar initial condition with reference model. These results also show the phenomenon of brittle deformation at the footwall during extreme extension as disused in the main text. The model can match the observations (Fig. 1b) in the first order (asymmetric structure, width of margins), but not in the fault-block scale.

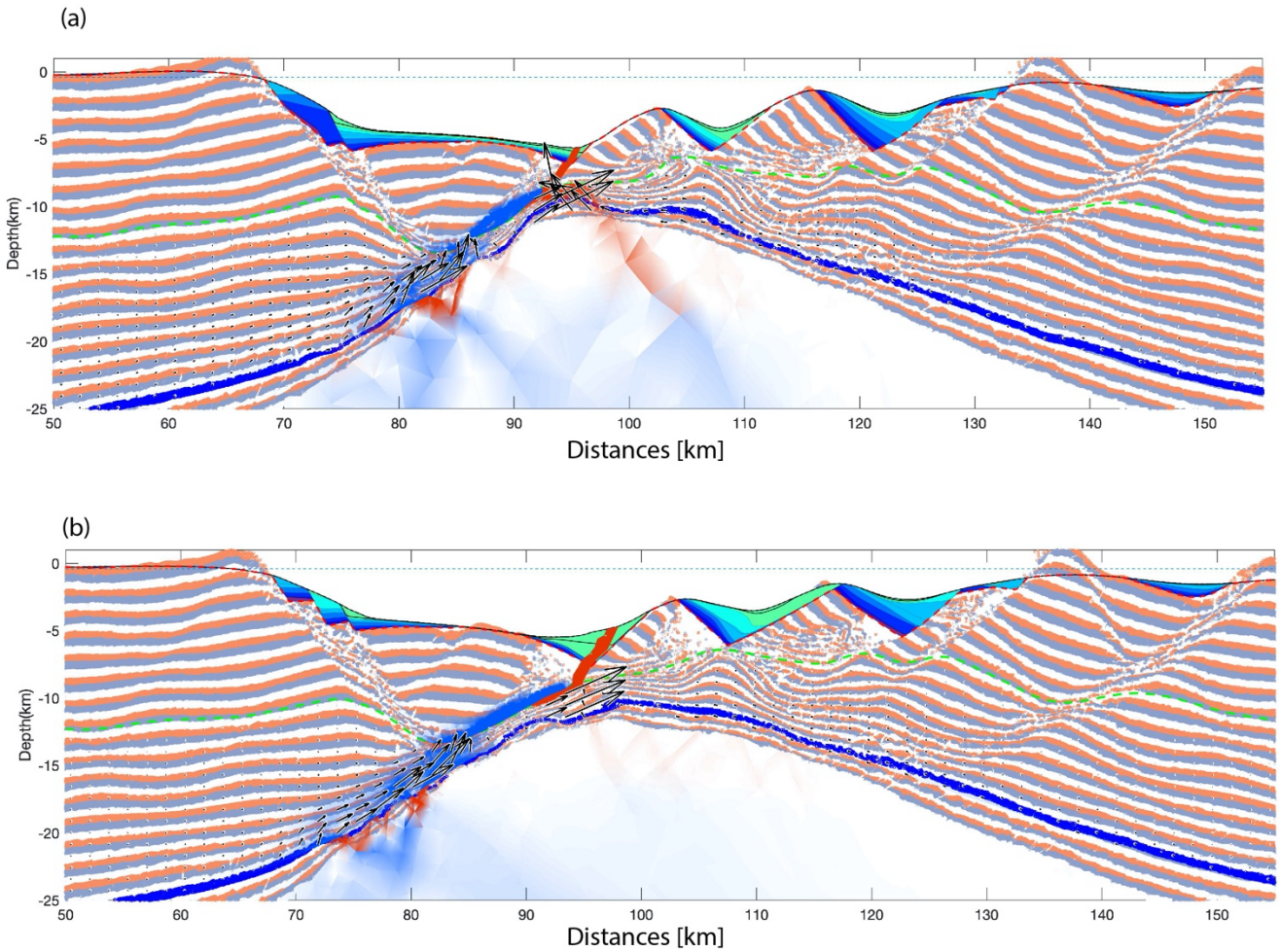

Fig. S8. Two models with different model resolution. (a) Model result with high-resolution upper crust. The resolution of the upper crust is 400 m, while lower crust resolution is 1000 m. (b) model result with the same resolution of upper and lower crust. The resolution of whole crust is equal to 600 m.

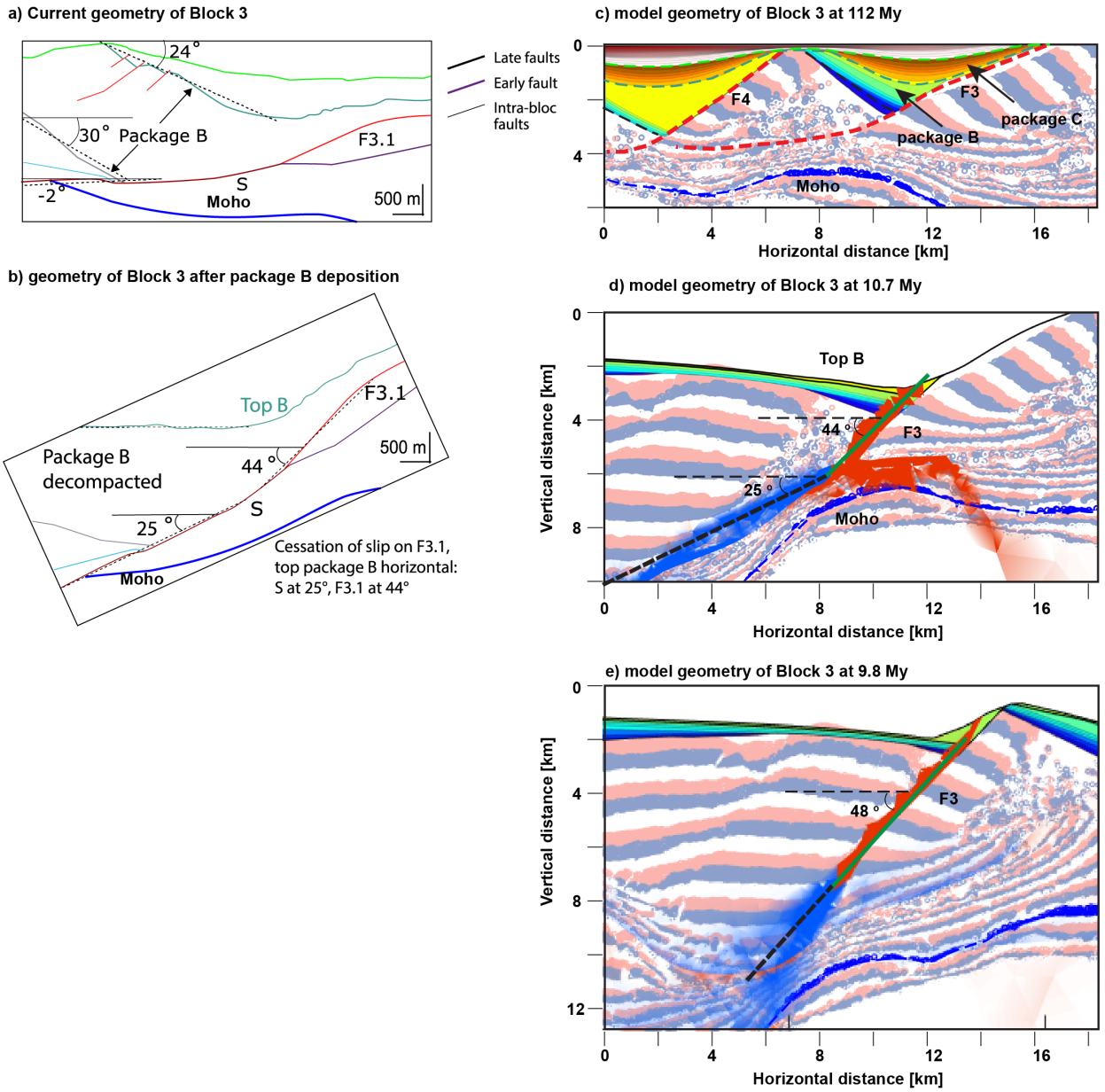

Fig. S9. Comparison between stratigraphic interpretation and modelling results on the slip angle of F3. (a) the final geometry of the stratigraphy on the top of block 3 along IAM11, from (Lymer et al., 2019). (b) geometry after package B deposition and assuming the top of package B was deposited horizontally (after Lymer et al., 2019). (c)-(e) the evolution of modelled F3. Interpreted angles during slip of fault F3, (b), are the same as those obtained during the model run (d).

Table S1. Model parameters.

Thermomechanical parameters					
Variable [unit]	Wet Quartzite	Wet Anorthite	Mafic Granulite	Dry Olivine	Wet Olivine
Dislocation pre-exponential factor $\log(B_{dis})$ [Pa^{-n} S^{-1}]	-28.0	-15.4	-21.05	-15.96	-15.81
Dislocation exponent n_{dis}	4.0	3.0	4.2	3.5	3.5
Dislocation activation energy E_{dis} [kj/mol]	223	356	445	530	480
Dislocation activation volume V_{dis} [10^{-6} m^3/mol]	-	-	-	13	10
Diffusion pre-exponential factor $\log(B_{dif})$ [Pa^{-n} S^{-1}]	-	-	-	-8.16	-8.64
Diffusion exponent n_{dif}	-	-	-	1	1
Diffusion activation energy E_{dif} [kj/mol]	-	-	-	375	335
Diffusion activation volume V_{dif} [10^{-6} m^3/mol]	-	-	-	6	4
Shear Modulus μ [GPa]	36	40	74	74	74
Thermal conductivity K [Wm^{-1} K^{-1}]	2.1	2.5	3.3	3.3	3.3
Heat capacity C_P [J kg^{-1} K^{-1}]	1200	1200	1200	1200	1200
Radiogenic heat production H_r [uWm^{-3}]	1.3	0.2	0	0	0
Bulk density ρ [kg m^{-3}]	2700	2850	3300	3300	3300
Thermal expansivity coefficient α [10^{-5} K^{-1}]	2.4	2.4	3.0	3.0	3.0
Initial cohesion (MPa)	10	10	10	10	10
Initial friction angle (°)	30	30	30	30	30
Surface process parameters					
Subaerial hillslope diffusion, K_L [m^2/year]	0.25				
Subaerial discharge transport coefficient α	$5 \cdot 10^{-4}$				
Submarine diffusion coefficient, Ks [m^2/year]	10^2				
Submarine diffusion coefficient decay, λ_s [m^{-1}]	$5 \cdot 10^{-4}$				
Pelagic sediment rate, C_S [m/year]	$1\ e^{-5}$ for syn-rift; $1e^{-6}$ for post-rift.				

Movie S1: Model evolution with total lower crust flow velocity. (a) thinning factor distribution along the model, orange solid line for lower crust, blue solid line for upper crust, purple dash line for whole crust and pink dash line for lithospheric mantle. (b) –(c) model evolution at different scales. Black arrows show the velocity of lower crust. Other legends and coloring as in Figure.5.

Movie S2: Model evolution with relative lower crust flow velocity. (a) thinning factor distribution along the model, orange solid line for lower crust, blue solid line for upper crust, purple dash line for whole crust and pink dash line for lithospheric mantle. (b) –(c) model evolution at different scales. Black arrows show the velocity of lower crust relative to upper crust. Other legends and coloring as in Figure.5.